

# SIMULTANEOUS DETECTION OF LONGITUDINAL AND TRANSVERSE BUNCH SIGNALS AT ANKA

B. Kehrer\*, E. Blomley, M. Brosi, E. Bründermann, N. Hiller†, A.-S. Müller, M. J. Nasse  
 M. Schedler, P. Schönfeldt, M. Schuh, P. Schütze‡, N. Smale, J. L. Steinmann, KIT, Karlsruhe, Germany

## Abstract

The ANKA storage ring offers different operation modes including the short-bunch mode with bunch lengths tuned down to a few picoseconds. This can lead to the occurrence of micro-bunching instabilities coupled to the emission of coherent synchrotron radiation (CSR) in so-called 'bursts'. To study this CSR instability we use several turn-by-turn enabled detector systems to synchronously measure both the THz signal as well as bunch profiles. The different detectors are placed at different locations around the storage ring. Here we discuss the experimental setup and calibration of the various systems' synchronisation.

## OVERVIEW

During the short bunch mode offered at the ANKA storage ring the momentum-compactness factor  $\alpha_c$  is lowered and thus the bunch length is reduced as well ('squeeze'). This is also coupled to the emission of coherent synchrotron radiation (CSR) and the occurrence of micro-bunching instabilities as long as the bunch current is above the instability threshold. The study of the CSR sets some requirements to the diagnostics: The response time and repetition rate must be sufficient to study a single bunch in a multi-bunch environment on a single-turn base. The acquisition time range should be long enough to cover the relevant time scales (up to some milliseconds). During the last years several detector systems have been installed and commissioned. They recently have been enabled to measure the bunch signatures synchronously. Here we focus on three different systems: A fast-gated intensified camera (FGC) to measure the horizontal bunch profile, the KAPTURE system to record signals from fast THz detectors and the electro-optical bunch profile monitor (EOSD) to record the longitudinal bunch profile.

### Fast-gated Intensified Camera (FGC)

The fast gated camera setup [1] that is used to monitor the horizontal bunch profile is located at the visible light diagnostics port [2]. It consists of a fast-gated intensified camera and a galvanometric mirror. This mirror is used to sweep the incoming incoherent synchrotron radiation over the CCD sensor before it is read out. The image intensifier in front of the CCD sensor is gated and thus allows to pick one bunch out of a multi-bunch fill. In case of ANKA the repetition rate of the gate allows to monitor up to every 6th turn. The voltage ramp for the mirror driver and the corresponding trigger signals for the camera are controlled

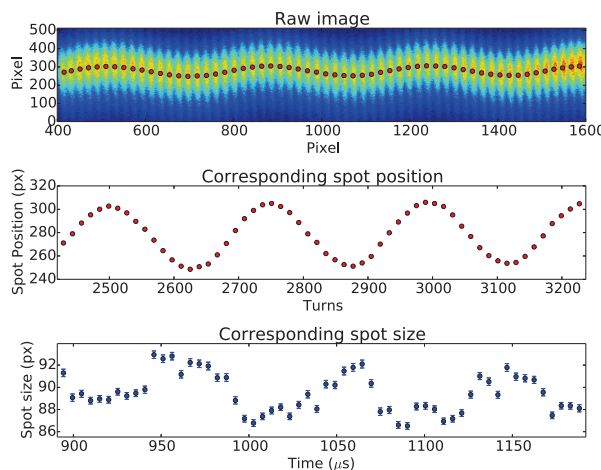


Figure 1: Sample picture from the fast-gated intensified camera (FGC). Top: raw data showing images of the same bunch for every 14th turn. Middle: centroid positions from 2D Gaussian fits plotted as a function of turns showing a synchrotron oscillation with  $f_s$  (synchrotron frequency). Bottom: Corresponding spot size versus time. The turn and time axes have their origin at the first revolution trigger after the measurement trigger.

via an arbitrary waveform generator. With this setup it is possible to place up to 65 spots (each spot corresponds to one single turn) on the sensor. The raw data from the CCD is processed by applying a 2D Gaussian fit to each spot to determine the horizontal bunch position and size, a sample picture is shown in Fig. 1.

### KAPTURE

The KAPTURE system is a FPGA-based read-out system to sample fast (THz-) detectors on a turn-by-turn and bunch-by-bunch base [3]. It consists of four ADCs that allow either to sample one detector with a local sampling rate of more than 300 GS/s or four detectors in parallel once per bunch and turn. For the investigation of the CSR intensity we use several detector systems such as Schottky diodes or a hot electron bolometer. Figure 3 shows an example of data taken with this system where we used two Schottky diodes to detect the CSR and one avalanche photo diode (APD) to measure the incoherent synchrotron radiation in the visible range.

### Electro-optical Spectral Decoding (EOSD)

At ANKA we use a streak camera and the principle of electro-optical spectral decoding (EOSD) to measure the longitudinal bunch profile. The EOSD setup is based on

\* benjamin.kehrer@kit.edu

† now at PSI, Villigen, Switzerland

‡ now at DESY, Hamburg, Germany

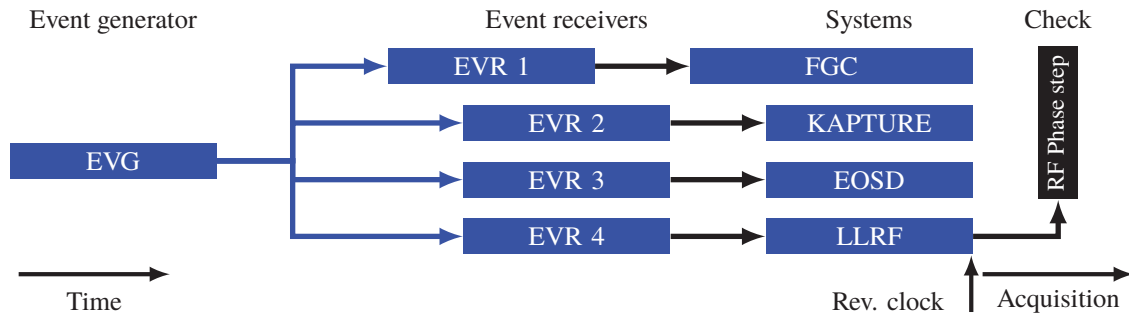


Figure 2: Scheme of the synchronization based on the ANKA timing system consisting of one event generator (EVG) and several event receivers (EVRs) located at the different setups. The intrinsic delay times of the setups are illustrated by different widths of the boxes and are compensated by the timing of the event receivers. The synchronisation is calibrated by a triggered RF phase step using the low-level RF system (LLRF).

an electro-optical crystal that is inserted into the beam pipe to sample the electric field of the bunch [4]. The crystal becomes birefringent due to the electric field and thus the linear polarisation of a long chirped laser pulse that is sent through the crystal is turned elliptical. This leads to a modulation of the laser pulse spectrum that is recorded using a spectrometer. The spectrometer is based on KALYPSO, an ultra-fast FPGA based DAQ-system [5] with a 256-pixel line array. This allows to record the longitudinal bunch profile for every turn. Additionally it is possible to measure the arrival time of the bunch. This will be later used for the calibration of the synchronisation.

## SYNCHRONISATION

The different setups described above are synchronised using the ANKA timing system [6]. We applied a common measurement trigger acting as an "arm trigger". The data acquisition directly starts with the next trigger pulse from the revolution clock. The synchronisation scheme illustrated in Fig. 2 takes the different delays of the experiments into account.

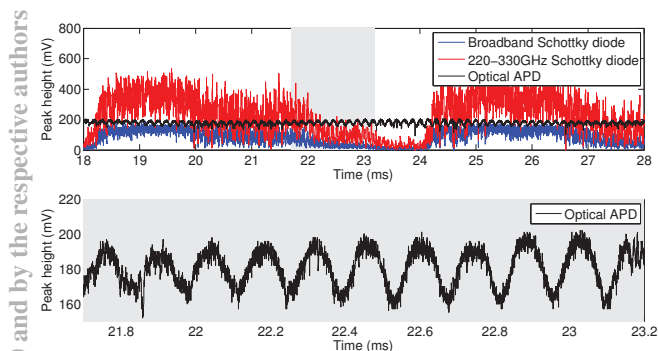


Figure 3: Time-domain signals recorded using KAPTURE connected to two Schottky diodes with different bandwidths (blue and red curve) and an optical avalanche photodiode (APD). The Schottky data show the saw-tooth like pattern that is characteristic to the occurrence of bursting. The bottom plot is a detail of the APD signal for the grey range showing a modulation with the synchrotron frequency.

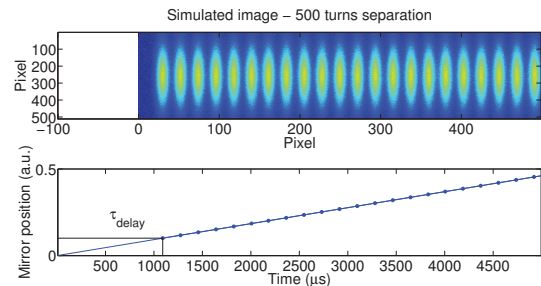


Figure 4: Illustration of the intrinsic delay time  $\tau_{\text{delay}}$  at the fast-gated intensified camera as the mirror is driven into a position where the light hits the CCD sensor.

The KAPTURE and the KALYPSO systems are based on the same hardware architecture allowing a quasi-instantaneous start of the detector read-out as the corresponding detectors sample continuously and independent of the read-out system. For the FGC there is a significantly longer preparation time required. It starts with the calculation of the voltage ramp in the waveform generator (depending on the chosen time range) that is then fed to the mirror driver. To save the CCD from overexposure the mirror has a hold position that reflects the light besides the CCD sensor. The light spot has to be driven onto it to start the measurements as illustrated in Fig. 4.

To confirm the synchronisation we used the low-level RF system (LLRF) to trigger a step in the RF cavity phase. The signature of such a step can be seen on all detector systems as it triggers a strong synchrotron oscillation of the bunch.

Figure 5 shows the successful synchronisation, as the RF phase step and its effects occur at the same turn for each system. For the synchrotron oscillation the FGC and KAPTURE are in phase. Compared to the maximum position from the electro-optical spectral decoding the phase difference is  $\pi/2$ . This is due to the fact that the projections of a rotation in the longitudinal phase space onto the position (x) and energy axis (y) are phase shifted by  $\pi/2$ . The FGC and KAPTURE are measuring the projection onto the energy axis (due to dispersion at the radiation source point)

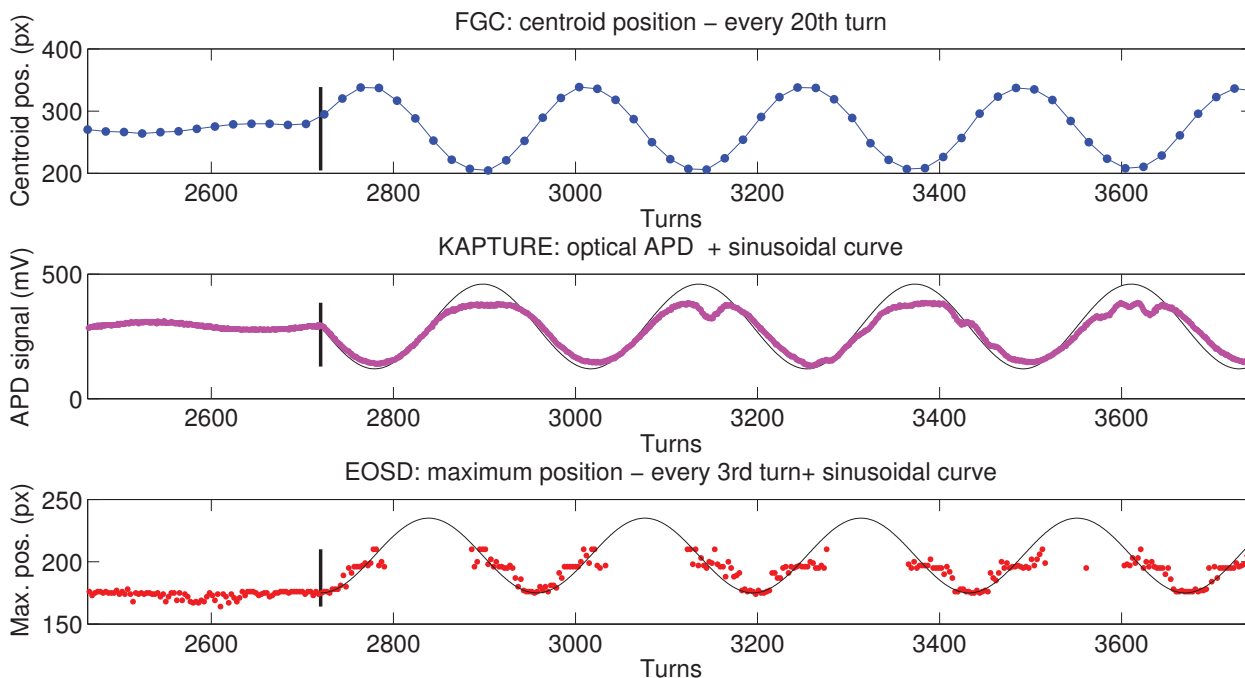


Figure 5: Signature of a triggered RF phase step on the different detector systems. Top: Horizontal centroid position recorded by the FGC. Middle: Peak amplitude for the optical APD recorded with KAPTURE, the black curve is a sinusoidal function with the synchrotron frequency  $f_s$  to illustrate the synchrotron oscillation. Bottom: EOSD maximum position as measure for the bunch arrival time (see Fig. 6), the black curve is also a sinusoidal curve with  $f_s$ . The thick, vertical black line in all plots shows the occurrence of the RF phase step. While the FGC and the signal from KAPTURE are in phase, the EOSD maximum position is phase shifted by a quarter synchrotron period.

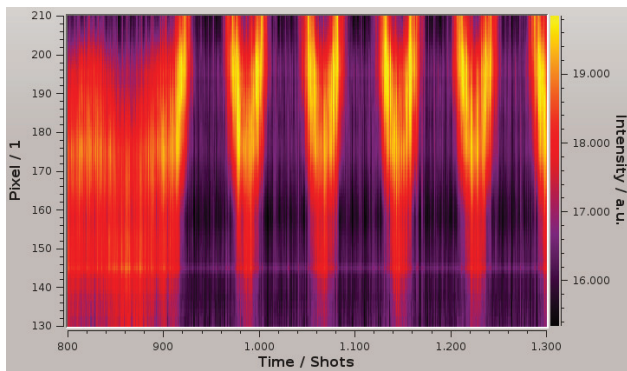


Figure 6: Raw image from the electro-optical spectral decoding (colour-coded longitudinal profiles displayed as a function of shots with a shot every third turn) showing the RF phase step. This step leads to the onset of a synchrotron oscillation and also a baseline shift due to the new RF phase. Due to the finite length of the laser pulse the upper part of the sinusoidal curve is cut.

while the electro-optical spectral decoding is sensitive to the projection onto the time / position axis by measuring also the arrival time.

### SUMMARY

With the different detector systems presented here we are able to record horizontal as well as longitudinal bunch

profiles and the CSR emission with a single turn and a single bunch resolution. By applying a common measurement trigger using the ANKA timing system we are now able to measure these beam properties synchronously. This synchronisation has been confirmed by using the low-level RF system to induce RF phase step.

### ACKNOWLEDGEMENTS

We would like to thank Anton Plech, Yves-Laurent Mathis and the ANKA IR-group for their support. This work has been supported by the Initiative and Networking Fund of the Helmholtz Association under contract number VH-NG-320 and by the BMBF under contract number 05K13VKA.

### REFERENCES

- [1] P. Schütze et al., in *Proc. IPAC'15*, MOPHA039, pp. 872-875
- [2] B. Kehrer et al., in *Proc. IPAC'15*, MOPHA037, pp. 866-868
- [3] M. Caselle et al., in *Proc. IBIC'14*, MOCZB1, pp. 24-28
- [4] N. Hiller et al., in *Proc. IPAC'13*, MOPME014, pp. 500-502
- [5] L. Rota et al., in *Proc. IBIC'14*, TUPD10, pp. 435-437
- [6] A. Hofmann et al., in *Proc. IPAC'10*, MOPD094, pp. 924-926